Proceedings of the 17th World Congress
The International Federation of Automatic Control
Seoul, Korea, July 6-11, 2008

Arm-side evaluation of ILC applied to a six-degrees-of-freedom industrial robot ⋆

Johanna Wallén * **Mikael Norrlöf** * **Svante Gunnarsson** *

* *Division of Automatic Control, Department of Electrical Engineering, Linköping University, SE-58183 Linköping, Sweden, (e-mail:* {johanna, mino, svante}@isy.liu.se*).*

Abstract: Experimental results from a first-order ILC algorithm applied to a large-size six-degrees-of-freedom commercial industrial robot are presented. The ILC algorithm is based on measurements of the motor angles, but in addition to the conventional evaluation of the ILC algorithm based on the motor-side error, the tool-path error on the arm side is evaluated using a laser-measurement system. Experiments have been carried out in three operating points using movements that represent typical paths in a laser-cutting application and different choices of algorithm design parameters have been studied. The motor-angle error is reduced substantially in all experiments and the tool-path error is reduced in most of the cases. In one operating point, however, the error does not decrease as much and an oscillatory tool behaviour is observed. Changed filter variables can give worse error reduction in all operating points. To achieve even better performance, especially in difficult operating points, it is concluded that an arm-side measurement, from for example an accelerometer, needs to be included in the learning.

Keywords: Iterative methods, Learning control, Control applications, Industrial robots, Position control.

1. INTRODUCTION

In many industrial robot applications the same trajectory is repeated over and over again. In such cases the *Iterative Learning Control* (ILC) method is a way to compensate for repetitive errors. The origin of ILC can be traced back to a US patent on "Learning control of actuators in control systems" (Garden, 1971). The first academic contribution to what today is called ILC is Uchiyama (1978), published in Japanese. From an academic perspective it was not until 1984 that ILC started to become an active research area, when Arimoto et al. (1984), Casalino and Bartolini (1984) and Craig (1984) independently described a method that iteratively compensated for model errors and disturbances. The development of ILC stems originally from the robotics area, and examples of contributions where ILC is applied in robotics are Arimoto et al. (1984), Bondi et al. (1988), Guglielmo and Sadegh (1996), and more recent works like Hätönen et al. (2004) and Butcher et al. (2008). The ILC research field is covered in surveys, like Moore (1999), Bristow et al. (2006) and Ahn et al. (2007).

This paper concern a relevant problem in laser cutting, and the purpose is to present results from experiments carried out on all six motors of a large-size commercial industrial robot. The experiments are performed using an ABB robot with an experimental controller, accomplishing a small circular movement in three different operating points. A commercial robot with similar load capacity (175 kg) is shown in Fig. 1. The robot positions used in the experiments are relevant for the application and they are chosen to avoid singularities, where the accuracy degrades.

⋆ This work was supported by the Swedish Research Council (VR).

The ILC algorithm applied to the robot is simple, see Sec. 3.1, where the choice of ILC algorithm and its design variables ω_n, δ and γ are motivated. The same ILC design variables are used for all six motors and the learning is stopped after five iterations. In practice there is little time for algorithm tuning and a small effort that gives a substantial error reduction after only a few iterations is often sufficient. Among the large number of publications dealing with various aspects of ILC, there are to the best knowledge of the authors very few publications presenting results of this kind, *i.e.*, studies where an ILC algorithm is applied to a real industrial robotic platform. In Longman (2000) and Elci et al. (2002) ILC is applied to a seven-

Fig. 1. Example of a large-size commercial industrial robot from ABB Robotics (2007) with similar size as the robot used in the experiments.

degrees-of-freedom robot arm, however smaller than the one used here, and the type of trajectories used in these experiments are not motivated by any particular application. Hakvoort et al. (2008) relies on accurate models of the robot and controller, which is not necessary here.

2. PROBLEM DESCRIPTION

This paper investigates the possibilities of an ILC algorithm applied onto a commercial robot system. Normally the motor angles are the only variables that can be measured in a commercial robot and therefore the algorithm has to be based on only them. The main purpose of the paper is to illustrate the difficulties that arise when the robot is subject to mechanical flexibilities and the ILC algorithm is based on motor-angle measurements only. This line of reasoning is motivated by a two-mass model of the dynamics of a single robot joint. Experimental results show that convergence of the ILC algorithm does not necessarily mean good performance on the arm side, *i.e.*, the position and orientation of the robot tool.

2.1 ILC applied to the robot system

Assuming that the mechanical flexibilities are concentrated to the robot joints, the simplified linear model of a single joint, shown in Fig. 2, can be used to explain the problem. The variable $q_m(t)$ denotes the motor angle, which is the only variable that is measured in commercial industrial robots. This variable is also used in the ILC algorithm when computing the update signal. However, the robot performance on the arm side is determined by the arm angle $q_a(t)$, which is not measured in the system.

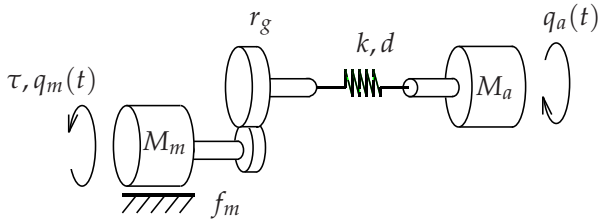

Fig. 2. A flexible two-mass model of a single robot joint, characterised by spring k, damper d, viscous friction f_m, gear ratio r_g, moments of inertia M_m, M_a, torque τ, motor angle $q_m(t)$ and arm angle $q_a(t)$.

In Sec. 4 it will be illustrated that convergence of the ILC algorithm and good performance when considering the motor-side error, calculated by the difference between motor-angle reference and measured motor-angle, does not necessarily imply high accuracy of the movement of the tool. Assuming that correct kinematic and dynamic models are available, the position and orientation of the tool could theoretically be derived from the motor angles. This is however not realistic, since it would require exact descriptions of phenomena like friction, backlash, motor torque ripple and nonlinear stiffness in the gearboxes, together with a complete model of the mechanical flexibilities. A remedy for handling this situation could be to use additional sensors and estimate the position and orientation of the tool. In the experiments presented in this paper the performance of the tool is measured using the laser-measurement system LTD500 from Leica Geosystems (2007). Since this is an expensive equipment, it is however only used in special applications, like Gunnarsson et al. (2006), where measurements are used in the ILC algorithm. For conventional operation it is preferable to use additional sensors, like accelerometers, in combination with signal processing algorithms to obtain accurate estimates of the relevant signals (Norrlöf and Karlsson, 2005). Future work is to use these estimates in the ILC algorithm.

2.2 General first-order ILC algorithm

The update equation for a general first-order ILC algorithm with iteration-independent operators is given by

$$u_{k+1}(t) = Q(q)\big(u_k(t) + L(q)e_k(t)\big), \tag{1}$$

where the subscript k denotes iteration number and q is the time-shift operator. The error

$$e_k(t) = r(t) - y_k(t), \tag{2}$$

is the difference between motor-angle reference signal and measured motor angle at iteration k. The update equation (1) implies the standard frequency-domain convergence criterion, see, *e.g.*, Norrlöf and Gunnarsson (2002a),

$$|1 - L(e^{i\omega})T_u(e^{i\omega})| < |Q^{-1}(e^{i\omega})|, \quad \forall\omega, \tag{3}$$

where T_u denotes the transfer function from the applied ILC input $u_k(t)$ to the measured output $y_k(t)$. The criterion shows that the filter Q can be used to improve the robustness of the ILC algorithm. The inequality (3) can be satisfied by choosing the magnitude of the Q filter small enough, and it is well known that this will prevent the final error to be zero, when the ILC algorithm has converged (Elci et al., 2002).

3. EXPERIMENTS

The ILC algorithm used in the experiments and the robot conditions are described more extensively. Thereafter the performance measures on the motor side and the arm side used in this paper are explained.

3.1 Experimental conditions

The robot is a multivariable system, but for simplicity the joints will be treated individually with a separate ILC algorithm for each joint. The algorithm is based on a heuristic design procedure, described in Norrlöf and Gunnarsson (2002b), which suggests a linear low-pass discrete-time Q filter and a linear discrete-time filter $L(q) = \gamma q^{\delta}$. Note that both filters can be non-causal. The general ILC algorithm (1) now implies the update equation

$$u_{k+1}(t) = Q(q)\big(u_k(t) + \gamma e_k(t+\delta)\big). \tag{4}$$

The design variables in the algorithm (4) are

- Type and order of the Q filter.
- Q filter cutoff frequency ω_n.
- Learning gain γ, with $0 < \gamma \leq 1$.
- Time shift δ of the filter L.

In this paper the design variables ω_n and δ and their influence of the ILC algorithm performance are investigated, while the other design variables remain constant during the experiments. Q is chosen as a second-order Butterworth filter, which is applied using the MATLAB

function `filtfilt` to get a zero-phase behaviour. The L filter gain γ is 0.9, motivated by the trade-off between convergence rate and robustness.

During the experiments the robot controller works in parallel with the ILC algorithm, *i.e.*, ILC works as a complement to the conventional system and can be implemented without modifying the controller. The update $u_k(t)$ from the ILC algorithm (4) is added to the reference signal of the control system (serial ILC architecture). The same ILC design variables are applied to all motors and the learning is stopped after five iterations, because an approach as simple as possible is desirable, see Wallén (2008).

The experiments are performed in the robot positions

$$\begin{aligned} p_1 &= (1.3166\ 0.0014\ 1.5992)\,, \\ p_2 &= (1.8000\ 0.1000\ 1.5992)\,, \\ p_3 &= (2.2000\ 0.2000\ 1.5992)\,, \end{aligned} \tag{5}$$

which correspond to the tool centre point (TCP) positions in meters, expressed in the robot base frame. The quaternion describing the orientation of the tool is identical in all three positions and all experiments. It is given by

$$q = (0.6322\ 0.0353\ 0.7732\ 0.0353)\,. \tag{6}$$

The robot configurations for the positions (5) can be seen in Fig. 3. The positions are relevant for the laser-cutting application because they are chosen to avoid singularities in the workspace of the robot and chosen not too far away from the zero pose in order to achieve good accuracy.

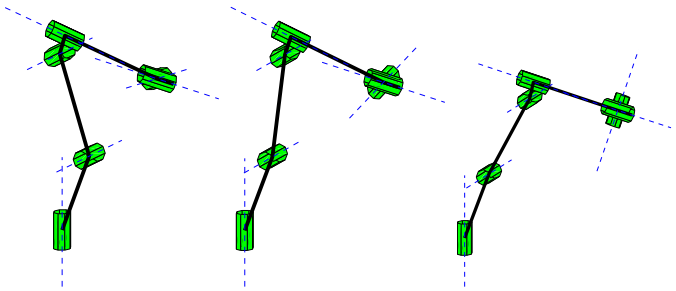

Fig. 3. The robot TCP positions (5) used in the experiments; p_1 (left), p_2 (centre), and p_3 (right).

In each position the robot makes circles of radius 5 mm with velocity $v = 40$ mm/s, using different filters Q and L to examine the performance and robustness of the ILC algorithm. In each set of experiments, one of the ILC design variables δ and ω_n varies, while the other remains constant. In Wallén et al. (2007) similar experiments were performed and evaluated on the motor side of the robot. Even though a fairly simple ILC algorithm was used in that work, it was shown that the reduction of the motor-angle error was substantial after only five iterations and the algorithm showed good robustness properties on the motor side, which is also the case here.

3.2 Performance measures

Motor side The results on the motor side are evaluated by the norm of the control errors for each iteration, normalised with respect to the largest control error without ILC for all motors and the experiments compared, as in

$$J_{k,i,j} = \frac{\|e_{k,i,j}\|}{\max_{l,m} \|e_{0,l,m}\|}. \tag{7}$$

The motor angle error (2) is denoted e and the subscripts $i = 1, \ldots, 6$ is motor number, j is experiment number and k denotes the iteration. The largest error for motor l in experiment m when no ILC algorithm is applied ($k = 0$) is used as a normalisation constant. One experiment means that one combination of operating conditions (position) of the robot and ILC design variables (δ, ω_n) is studied. The error measure (7) is studied using 2-norm and ∞-norm.

Arm side The root mean square (RMS) error on the arm side for experiment number j at iteration k is

$$\mathrm{RMS}_{k,j} = \sqrt{\frac{1}{N} \sum_n \big(r_{ref} - r_{meas,k}(n)\big)^2}, \tag{8}$$

where $r_{meas,k}(n)$ denotes the radius of the measured circle for each sample n, and N is the total number of samples along the circle. The maximum deviation (maxdev) from the reference circle r_{ref} for experiment j at iteration k is defined as

$$\mathrm{maxdev}_{k,j} = \max_n \big(|r_{ref} - r_{meas,k}(n)|\big). \tag{9}$$

The error measures (8)–(9) when several experiments j are compared, are normalised with the experiment m with the largest error without ILC, according to

$$\mathrm{RMS}_k = \frac{\mathrm{RMS}_{k,j}}{\max_m \big(\mathrm{RMS}_{0,m}\big)}, \tag{10}$$

$$\mathrm{maxdev}_k = \frac{\mathrm{maxdev}_{k,j}}{\max_m \big(\mathrm{maxdev}_{0,m}\big)}. \tag{11}$$

4. EXPERIMENTAL RESULTS

First the results for the "nominal" case, *i.e.*, $\delta = 3$ and $\omega_n = 10$ Hz, are shown for the operating positions (5). They are compared to the resulting robot performance in experiments with $\delta = 6$, $\omega_n = 10$ Hz and $\delta = 3$, $\omega_n = 15$ Hz, respectively.

4.1 Performance with respect to operating points

Experiments are performed in the three positions (5) with the ILC design variables $\delta = 3$ and $\omega_n = 10$ Hz. First, the result from experiments in p_1 is shown. This position gives a good learning, as can be seen in Fig. 4, where the circle measured on the arm side at each iteration is compared to an ideal reference circle with radius 5 mm. The motor-side errors are compensated for by the ILC algorithm and the circle on the arm side, measured by the Leica laser tracker LTD500, is close to the reference circle after five iterations.

In Fig. 5 the behaviour in the positions (5) on the motor side is evaluated, using the error measure (7) expressed in ∞-norm. The error measure (7) expressed in 2-norm shows a similar appearance, see Wallén et al. (2007). It is interesting to note that the motor-side errors, *i.e.*, the difference between reference and measured motor angles, are reduced in all three positions compared to when no ILC algorithm is applied. The only exception is motor 2 in position p_2, where a slightly increasing behaviour can be noticed after a few iterations. The low reduction of the errors for motors 1 and 5 in position p_3 is due to a high-frequency error component, which is above the cutoff frequency ω_n of the Q filter. Adjusting ω_n in this position

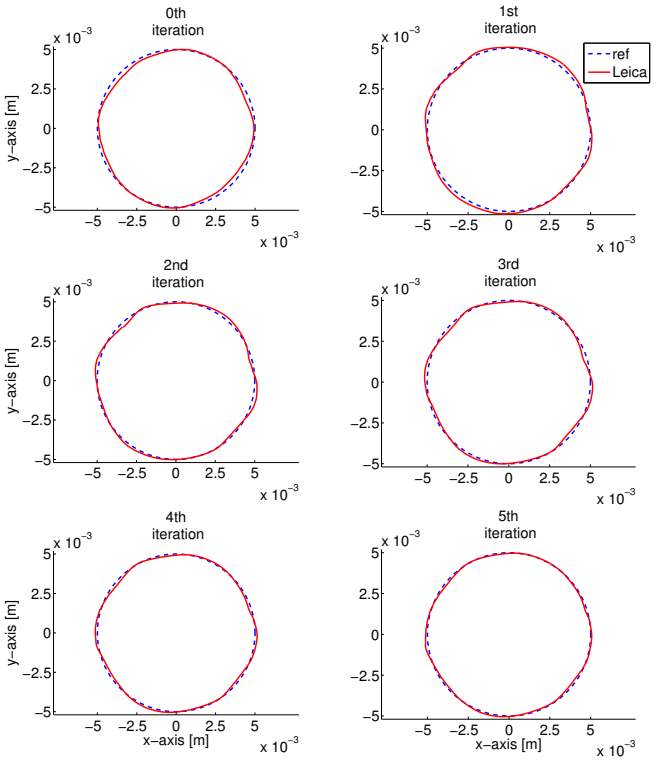

Fig. 4. Measured circles on the arm side at every iteration, compared to an ideal circle. The experiment is performed in position p_1 and with ILC design variables $\omega_n = 10\,\text{Hz}$ and $\delta = 3$. The experiment shows a good behaviour and the measured circle is close to the reference circle after five iterations.

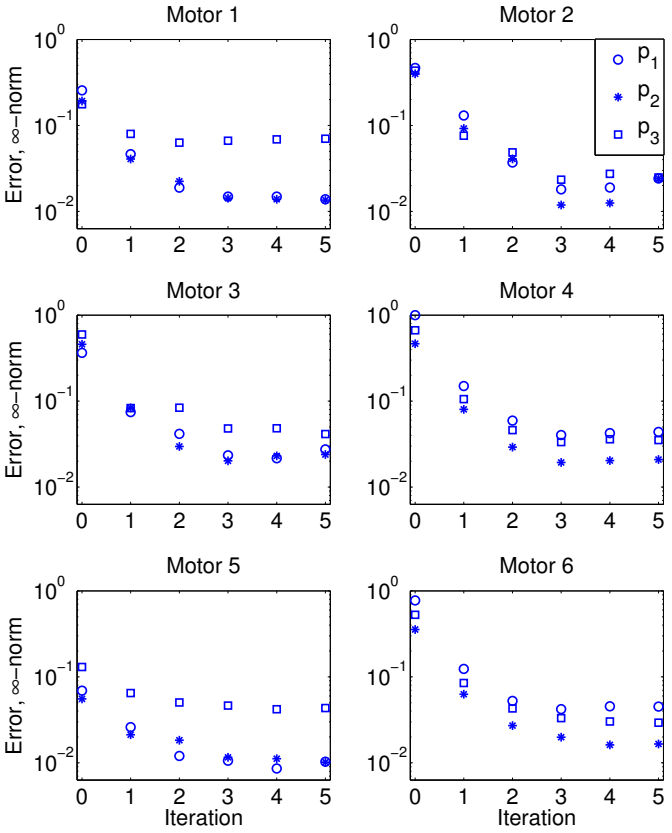

Fig. 5. The error measure $J_{k,i,j}$, see (7), on the motor side expressed in ∞-norm for all motors $i = 1, \ldots, 6$, three positions $j = p_1, p_2, p_3$ and iterations $k = 0, \ldots, 5$. The experiments are performed with the ILC design variables $\omega_n = 10\,\text{Hz}$ and $\delta = 3$ and shows a decreasing error for all positions.

can give a possibly reduced effect of this disturbance on the error. However, the conclusion in Fig. 5 is, viewed on the whole, a decreasing error for all positions at all iterations.

As a comparison, Fig. 6 shows the RMS error (10) and maximum deviation (11) of the error on the arm side for the three positions (5). The error measure (7) in 2-norm on the motor side corresponds to the RMS error on the arm side. The error measure (7) in ∞-norm on the motor side, seen in Fig. 5, corresponds to the maximum deviation of the error on the arm side. Position p_1 gives the best behaviour in Fig. 6, with a decreasing trend in both RMS error and maximum deviation of the error. This corresponds well to the result on the motor side, seen in Fig. 5. Position p_2 shows an increasing trend of the errors, and for position p_3, the errors are as large as or even larger as the errors at the 0th iteration, when no ILC algorithm is applied. Changing the filter parameters can give a worse error reduction also in the other positions. These results show that even though the result on the motor side is good, it is no guarantee that the performance on the arm side is improved. There are a number of possible explanations for the observed behaviour. First, the operating point plays an important role. A more extended robot makes the problem harder, because mechanical flexibilities become more pronounced in a more extended position. The fact that the arm-side error in point p_3 grows during the initial iteration can be a result of the externally injected ILC signal, which can excite the flexibilities.

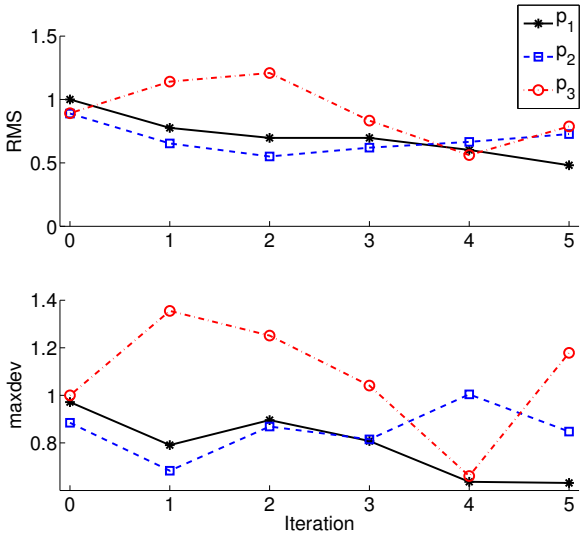

Fig. 6. The error measures on the arm side, see (10)–(11); RMS error and maximum deviation of the error for positions p_1, p_2 and p_3. In the experiment the ILC design variables $\omega_n = 10\,\text{Hz}$ and $\delta = 3$ are used.

4.2 Performance with respect to δ

The robot performance with respect to the time shift δ of the filter $L = \gamma q^{\delta}$ is investigated in experiments performed in positions p_1 and p_2. The ILC design variables $\delta = 3$ and 6 and cutoff frequency $\omega_n = 10\,\text{Hz}$ are used. In Fig. 7 it is seen that $\delta = 6$ gives lower RMS error (10) and maximum deviation (11) of the error on the arm side.The corresponding behaviour can also be seen on the motor side, see Wallén et al. (2007), explained by the fact that $\delta = 6$ theoretically gives a higher suppression of the error and thereby a faster convergence.

4.3 Performance with respect to ω_n

The robot performance with respect to the cutoff frequencies $\omega_n = 10$ and $15\,\text{Hz}$ has also been investigated. The experiments have been carried out with $\delta = 3$ in positions p_1 and p_2. A similar behaviour can be noticed for positions p_1 and p_2, therefore only results for p_1 are shown. When studying the error measure (7) on the motor side expressed in ∞-norm, see Fig. 8, the errors are reduced for $\omega_n = 15\,\text{Hz}$ compared to $\omega_n = 10\,\text{Hz}$. It can be explained by the fact that with a higher cutoff frequency of the Q filter, a larger part of the error signal is taken into account in the ILC update equation (4). However, the corresponding error measures (10)–(11) on the arm side, shown in Fig. 9, concludes that the actual tool-path error is increased for $\omega_n = 15\,\text{Hz}$ compared to $\omega_n = 10\,\text{Hz}$. This is an opposite result compared to Fig. 8, and will be discussed next.

An oscillatory behaviour on the arm side is noticed, as can be seen in Fig. 10, where the results from the 0th and 5th iteration are compared. The only difference between the

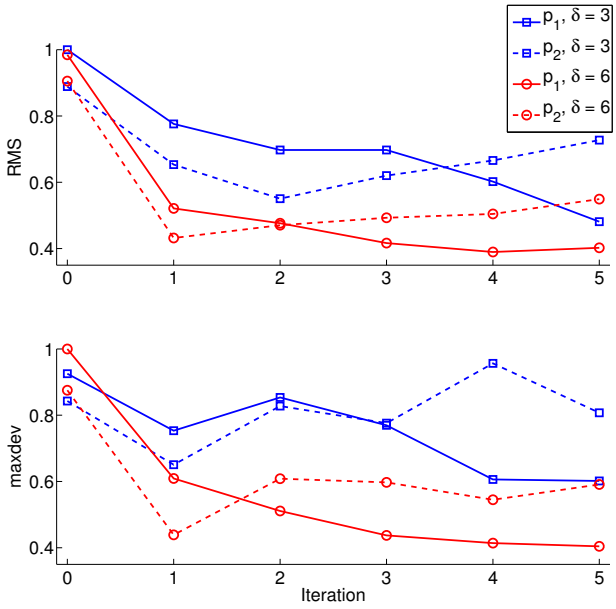

Fig. 7. The error measures on the arm side, see (10)–(11); RMS error and maximum deviation of the error for positions p_1 and p_2. The experiments are performed with the ILC design variables $\omega_n = 10\,\text{Hz}$ and $\delta = 3$ and 6. $\delta = 6$ gives lower errors, which is explained by decreasing energy content in the ILC update signal.

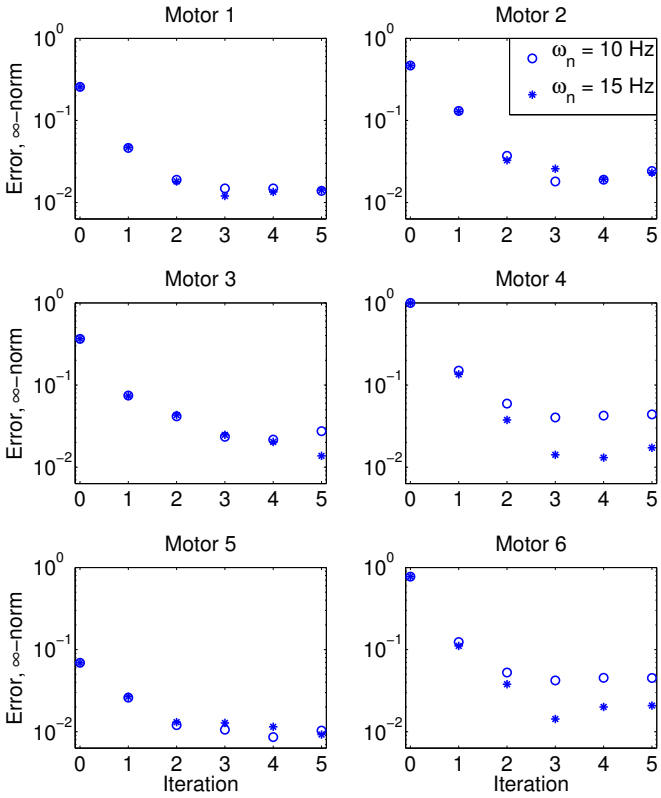

Fig. 8. The error measure $J_{k,i,j}$, see (7), on the motor side expressed in ∞-norm for all motors $i = 1, \ldots, 6$, cutoff frequencies $\omega_n = 10$ and $15\,\text{Hz}$ and iterations $k = 0, \ldots, 5$. The experiments are performed in position p_1 with $\delta = 3$. A higher cutoff frequency gives a better reduction of the control error, but the error is no longer monotonically decreasing as a function of iteration.

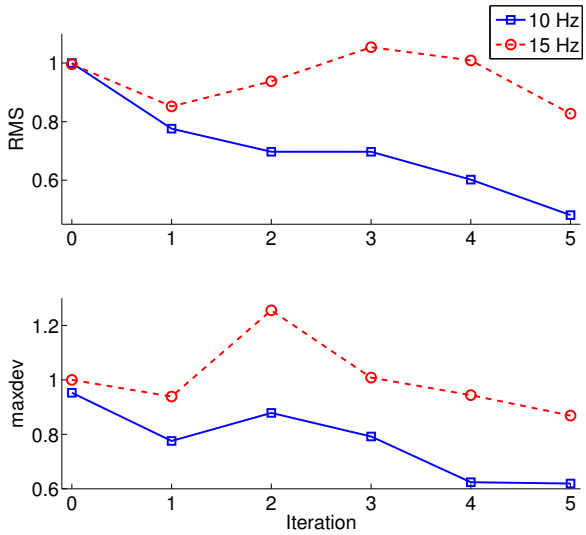

Fig. 9. The error measures on the arm side, see (10)–(11); RMS error and maximum deviation of the error for position p_1. The experiments are performed with the ILC design variables $\omega_n = 10$ and $15\,\text{Hz}$ and $\delta = 3$. Higher ω_n gives larger errors on the arm side.

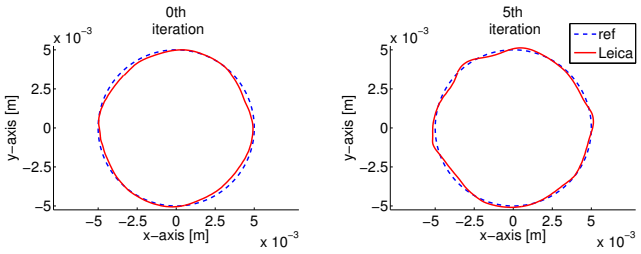

Fig. 10. Measured circle on the arm side when the experiment is performed in position p_1, with the ILC design variables $\delta = 3$ and $\omega_n = 15\,\text{Hz}$. Iteration 0 and 5 are compared and an oscillatory behaviour is noticed.

cases, is the ILC control signal added. When oscillations occur on the arm side after a few iterations, they originate from the ILC update signal u_k, applied at iteration k.

The message in this example with varying cutoff frequencies ω_n of the Q filter, is that one has to be very careful when dealing with resonant systems. The ILC algorithm can increase the oscillations in the system, in particular when the controlled variable, here the tool position, is not directly measured and included in the algorithm. It motivates the need of additional sensors, like accelerometers, to obtain accurate estimates of the arm-side movements and use this information in the algorithm.

5. CONCLUSIONS AND FUTURE WORK

A first-order ILC algorithm has been applied on a large-size commercial industrial robot with six degrees of freedom. The operating points represent typical robot configurations in a laser-cutting application. A heuristic ILC algorithm is used, based on the motor angles, and the same design variables are used for all six motors for simplicity reasons. The performance on the arm side is evaluated by a laser-measurement system and compared to the motor-side errors. It can be concluded that the tool-path error is reduced in most cases. However, the ILC algorithm can increase the oscillations in the resonant system because the motor angles are used in the algorithm, and not the actual tool position. To achieve even better performance, especially in difficult operation points, it is concluded that arm-side measurements from for example an accelerometer need to be included in the learning. Future work includes arm-side measurements combined with signal processing algorithms to obtain accurate estimates of the actual tool path. Some works in this direction are presented in Gunnarsson et al. (2007) and Norrlöf and Karlsson (2005).

REFERENCES

ABB Robotics, 2007. Open public archive of robot images. URL: `http://www.abb.se`, accessed December, 2007.

H.-S. Ahn, Y. Chen, and K. L. Moore. Iterative learning control: Brief survey and categorization. *IEEE Trans. Systems, Man, Cybernetics – Part C: Appl. Reviews*, 37(6):1099–1121, November 2007.

S. Arimoto, S. Kawamura, and F. Miyazaki. Bettering operation of robots by learning. *Journal Robot. Syst.*, 1(2):123–140, 1984.

P. Bondi, G. Casalino, and L. Gambardella. On the iterative learning control theory for robotic manipulators. *IEEE Journal Robot. Autom.*, 4:14–22, February 1988.

D. A. Bristow, M. Tharayil, and A. G. Alleyne. A survey of iterative learning control. *IEEE Control Syst. Mag.*, pages 96–114, 2006.

M. Butcher, A. Karimi, and R. Longchamp. A statistical analysis of certain iterative learning control algorithms. *Int. Journal Control*, 81(1):156–166, January 2008.

G. Casalino and G. Bartolini. A learning procedure for the control of movements of robotic manipulators. In *IASTED Sym. Robot. Autom.*, pages 108–111, San Francisco, USA, May 1984.

J. J. Craig. Adaptive control of manipulators through repeated trials. In *Proc. American Control Conf.*, pages 1566–1572, San Diego, CA, June 1984.

H. Elci, R. W. Longman, M. Q. Phan, J.-N. Juang, and R. Ugoletti. Simple learning control made practical by zero-phase filtering: Applications to robotics. *IEEE Trans. Circuits Syst. I, Fundam. Theory Appl.*, 49(6):753–767, June 2002.

M. Garden. Learning control of actuators in control systems. US Patent 03555252, January 1971. Leeds & Northrup Company, Philadelphia, USA.

K. Guglielmo and N. Sadegh. Theory and implementation of a repetetive robot controller with cartesian trajectory description. *Journal Dynamic Syst., Measurement Contr.*, 118:15–21, March 1996.

S. Gunnarsson, M. Norrlöf, G. Hovland, U. Carlsson, T. Brogårdh, T. Svensson, and S. Moberg. Pathcorrection for an industrial robot. US Patent 7130718, October 2006.

S. Gunnarsson, M. Norrlöf, E. Rahic, and M. Özbek. On the use of accelerometers in iterative learning control of a flexible robot arm. *Int. Journal Control*, 80(3):363–373, March 2007.

W. B. J. Hakvoort, R. G. K. M. Aarts, J. van Dijk, and J. B. Jonker. Lifted system iterative learning control applied to an industrial robot. *Control Eng. Practice*, 16(4):377–391, April 2008.

J. J. Hätönen, D. H. Owens, and K. L. Moore. An algebraic approach to iterative learning control. *Int. Journal Control*, 77(1):45–54, January 2004.

Leica Geosystems, 2007. URL: `http://www.leica-geosystems.com/ims/product/ltd.htm`, accessed August, 2007.

R. W. Longman. Iterative learning control and repetitive control for engineering practice. *Int. Journal Control*, 73(10):930–954, July 2000.

K. L. Moore. Iterative learning control - an expository overview. *App. Computational Controls, Signal Proc. Circuits*, 1:151–214, 1999.

M. Norrlöf and R. Karlsson. Position estimation and modeling of a flexible industrial robot. In *IFAC World Congress*, Prague, Czech Republic, 2005.

M. Norrlöf and S. Gunnarsson. Time and frequency domain convergence properties in iterative learning control. *Int. Journal Control*, 75:1114–1126, 2002a.

M. Norrlöf and S. Gunnarsson. Experimental comparison of some classical iterative learning control algorithms. *IEEE Trans. Robot. Autom.*, 18:636–641, 2002b.

M. Uchiyama. Formulation of high-speed motion pattern of a mechanical arm by trial. *Trans. Soc. Instr. Control Eng.*, 14(6): 706–712, 1978. Published in Japanese.

J Wallén. *On Kinematic Modelling and Iterative Learning Control of Industrial Robots.* Licenciate's Thesis no 1343, Dept. Electr. Eng., Linköpings universitet, Sweden, January 2008. Available: `http://www.control.isy.liu.se/research/reports/LicentiateThesis/Lic1343.pdf`.

J. Wallén, M. Norrlöf, and S. Gunnarsson. Experimental evaluation of ILC applied to a six degrees-of-freedom industrial robot. In *Proc. Eur. Control Conf.*, Kos, Greece, July 2007.